IJCCSM
18,1

Received 5 September 2025
Revised 22 October 2025
Accepted 28 October 2025

Analysis of photovoltaic power plant resilience under Iberian heatwaves

Sara Pereira, Henrique Miguel Fava Rica, Joana Correia, José A. Silva and Afonso Cavaco
Renewable Energies Chair, University of Évora, Évora, Portugal

Abstract

Purpose – This study aims to quantify heatwave impacts on operational performance of Iberian photovoltaic (PV) plants in the context of climate change and examines whether typical meteorological year (TMY) expectations mask event-driven losses. It isolates performance ratio (PR) degradation, timing and recovery, providing evidence to align PV deployment planning and operation and maintenance (O&M) with a warming climate.

Design/methodology/approach – Three plants (Spain: 2, Portugal: 1) are analysed at hourly and daily scales across pre/during/post-heatwave windows. PVsyst simulations are produced with TMY and ERA5-Land. ERA5-Land is benchmarked against a co-located station. Resilience metrics include PR drop, time-to-trough, recovery-to-90% and energy not served (ENS).

Findings – Heatwaves caused sharp hourly troughs (maximum 90.44%) but modest daily losses (largest 17.59%, Zebro-2P) with recovery within 0–1 days. TMY expectations overpredicted energy in all cases; the largest gap was 553.25 kWh (36.88 kWh/kWp; 17.3% of simulated energy) at Zebro-2P; the highest relative gap was 22.34% at Ariza-2S.

Research limitations/implications – The data is limited to three plants and four events, with *in situ* meteorology at one site.

Originality/value – This work introduces an auditable, event-centric PR stress test using *in situ*-validated ERA5 denominators, contrasting TMY counterfactuals, with drop/time-to-trough/recovery metrics and an ENS design-gap to translate heatwave impacts into operationally actionable insights for resilient PV design and O&M.

Keywords Heatwaves, Performance ratio, Photovoltaics, Portugal, Spain, Typical meteorological year

Paper type Research paper

1. Introduction

The ongoing climate change is producing significant impacts in all aspects of human life, with Europe at the epicentre of its impacts. Since 1979, Europe's surface air temperatures

Funding: This work has received funds from the European Union's Horizon 2020 research and innovation program under grant agreement No: 101036418.

This research has received funds from the European Union's LIFE program under grant agreement No: 101076395.

The work is also funded by national funds through FCT – Fundação para a Ciência e Tecnologia, I.P., in the framework of the UID/6478 – SOL4R Applied Research in Solar Energy for the Energy Transition.

This work uses information obtained, among other sources, from the Sistema de Información Agroclimática para el Regadío (SIAR), Ministerio de Agricultura, Pesca y Alimentación.

International Journal of Climate Change Strategies and Management
Vol. 18 No. 1, 2026
pp. 110-126
Emerald Publishing Limited
1756-8692
DOI 10.1108/IJCCSM-09-2025-0305

have increased about three times as fast as the global average, in both winter and summer (Dong and Sutton, 2025). This excess warming is largely due to greenhouse gas emissions, changes in aerosols and shifts in atmospheric circulation patterns that bring more warm air into Europe (Dong and Sutton, 2025; Vautard *et al.*, 2023). Regional projections confirm European land temperatures will continue to rise by 1.2–3.4°C under SSP1-2.6 and up to 8.5°C under SSP5-8.5 by 2100, with the strongest warming expected in northeastern Europe and inland areas of Mediterranean countries (EEA, 2025). As a result, the frequency, intensity and duration of extreme weather events, including heatwaves, floods, droughts, hailstorms, wildfires and high wind events, has increased (Vautard *et al.*, 2023; Ruosteenoja *et al.*, 2023). The 2022 summer was Europe's hottest summer, triggering the most severe drought in 500 years and widespread wildfires across Southern Europe (IPCC, 2022). Future projections indicate higher risks of pluvial flooding in Northern and Western-Central Europe, while Southern and Western-Central regions will face more frequent droughts and extreme heat, with populations enduring over 60 days annually above 35°C by century's end (IPCC, 2022).

Other hazards are also intensifying. Hail is already among the costliest weather-related events, with northern Italy recording up to 40 severe storms per 10,000 km^2 each year (EEA, 2021; Kahraman *et al.*, 2024). Climate simulations suggest hailstorm tracks could expand by 15%–30%, with doubled frequency of > 50 mm hailstones (Brennan *et al.*, 2025). Altogether, the financial burden of climate-related risks in Europe could reach €40bn annually by the 2080s, with €35bn attributable to heatwaves and droughts (IPCC, 2022). These changes already threaten energy infrastructure. Extreme events can reduce system reliability by up to 16% and grid integration capacity by 34% (Perera *et al.*, 2020). Both centralised and distributed generation are vulnerable, with building-level PV systems especially exposed during prolonged heatwaves or islanded operation (Han *et al.*, 2025). The economic losses amount to billions annually (Añel *et al.*, 2024), with low-income households disproportionately affected by energy poverty and price volatility (Lei and Xu, 2024).

Solar photovoltaics (PVs) play a dual role in Europe's energy transition: they are central to decarbonisation, with more than 339 GW installed by 2024 (IEA, 2025), yet are also highly exposed to climatic stressors. PV performance is sensitive to temperature, irradiance, aerosols, humidity and wind, many of which are shifting under climate change (Patt *et al.*, 2013; Bamisile *et al.*, 2025). Temperature is one of the most critical factors. Rising air temperatures reduce efficiency by 0.3%–0.5% per °C above 25°C (IEA, 2022), while heatwaves can drive module surface temperatures above 70°C, accelerating degradation (Islam *et al.*, 2024; Omazic *et al.*, 2019). Laboratory studies show crystalline silicon modules lose 0.46%–0.50% efficiency per °C, with heatwave conditions leading to 4%–10% efficiency drops between 35°C and 49°C (Razak *et al.*, 2016; Hudișteanu *et al.*, 2024). Thin-film technologies such as copper indium gallium selenide (CIGS) are less thermally sensitive, offering some advantages in very hot regions (Ebhota and Tabakov, 2022). Thermal stress also affects other system components. Expansion mismatches between polymers and encapsulants promote delamination and cracking (Meslier *et al.*, 2024). Inverters can derate or shut down once internal temperatures exceed design thresholds (De Lima *et al.*, 2023), while mounting structures deform under prolonged heat (Okonkwo *et al.*, 2025). Storage systems face reduced efficiency under elevated temperatures (Husain *et al.*, 2024). Beyond heat, PV systems are vulnerable to other extreme events. Hail can cause direct glass and cell damage, with losses up to 21.8% in thin-glass modules (Chakraborty *et al.*, 2023). Strong winds exceeding 200 km/h have detached modules from mounting structures, as observed in northern Italy, Slovenia and Croatia (Bošnjaković *et al.*, 2023). Conversely, moderate winds provide cooling benefits, lowering module temperature by

1–7°C depending on speed (Ataman and Arslanoğlu, 2024). Flooding of ground-mounted systems can erode foundations and damage electrical components, while dust storms increase module temperatures by 5°C and reduce efficiency by 25% after 30 days without cleaning, though up to 90% can be recovered after washing (Chen *et al.*, 2019). Wildfire smoke reduces irradiance significantly, cutting direct normal irradiance (DNI) by up to 42% and global horizontal irradiance (GHI) by up to 17% (Corwin *et al.*, 2025), while increased soiling due to ash accumulation or direct infrastructure damage also affect PV systems (Gilletly *et al.*, 2023; Ford *et al.*, 2024). These stressors also accelerate long-term degradation. Elevated temperatures, UV radiation and arid conditions degrade cables, seals and junction boxes, even when certified for outdoor exposure (IEA, 2022). Prolonged operation above 85°C risks irreversible damage to modules (Gahlot, 2024). In southern Spain and Portugal, degradation rates reach up to 0.8% per year (Ascencio-Vásquez *et al.*, 2019; Poddar *et al.*, 2024). Altogether, these factors compromise both short-term yield and system lifespan, highlighting the need for resilient design and adaptive operation and maintenance (O&M).

Despite the growing risks posed by climate extremes, a substantial gap persists between model-based climate projections and the operational performance of PV systems under stress. The most widely used input for PV yield simulations remains the typical meteorological year (TMY), which condenses long-term averages into a representative year. While useful for estimating typical annual production, TMY files cannot capture short-term anomalies or the dynamics of extreme events such as heatwaves, dust intrusions or wildfire smoke (Loon *et al.*, 2020). As a result, TMY-based simulations often overestimate energy yield and underestimate operational risk. Similarly, many techno-economic models fail to incorporate degradation, soiling or maintenance failures triggered by climatic stressors, further limiting their ability to inform adaptation planning (Hameed *et al.*, 2024). In response, recent literature emphasises the need for a more integrated perspective, bridging climate science, PV modelling and real-world performance analysis. This is reflected in the evolving paradigm of climate resilience, which stresses that solar infrastructure must not only be efficient under average conditions but also capable of withstanding and recovering from disruptive events (IEA, 2022).

We frame PV resilience along three complementary dimensions: resistance, the capacity of components to withstand physical stresses (e.g. hail, wind, heat) without damage (Bošnjaković *et al.*, 2023); robustness, the ability of the plant to sustain acceptable performance under adverse operating conditions (e.g. thermal derating, particulate-laden skies) (Jimba *et al.*, 2025); and recovery, the rapidity and completeness with which performance returns to pre-event levels after disruption (Bošnjaković *et al.*, 2023; Jimba *et al.*, 2025). Building on this framing, three methodological strands are common. Firstly, simulation studies based on TMY remain the baseline and are increasingly complemented with downscaled climate projections from CMIP6/CORDEX to sample future extremes (Rady *et al.*, 2025; Rettie *et al.*, 2023; Gutowski *et al.*, 2020). Secondly, empirical and data-driven analyses couple PV production with observations or reanalyses such as ERA5-Land to evaluate behaviour during real events, using statistical models (Kim *et al.*, 2019; Fregosi and Bolen, 2022), machine learning (Sun *et al.*, 2024; Zhang *et al.*, 2024) and/or digital twins (Pierce *et al.*, 2024). Thirdly, resilience is quantified with dynamic metrics such as resilience curves (Panteli *et al.*, 2017; Dehghani *et al.*, 2023), outage frequency and duration (Ekisheva *et al.*, 2022; Abdelmalak *et al.*, 2023), restoration rates, composite indices (Dwivedi *et al.*, 2025; Ghosh and De, 2022) and survivability metrics estimating the probability of maintaining critical loads (Pizzimbone and Jrad, 2023). While these advances represent important progress, most existing frameworks remain limited in addressing compound or

sequential hazards, which are increasingly common under climate change. Bridging this gap requires methodological innovation, region-specific calibration, improved access to high-resolution data and stronger integration of simulations with operational evidence.

As the frequency and intensity of climatic extremes increase, O&M practices become central to the resilience of PV systems. Traditional O&M frameworks, designed for relatively stable conditions, are insufficient when plants are exposed to heatwaves, floods, dust storms, hail and high winds. Preventive strategies, site-specific adaptation and rapid response protocols are essential to safeguard long-term reliability (IEA, 2022). Resilient O&M involves not only regular monitoring and inspections, such as infrared thermography, I–V curve testing and insulation quality assessments, but also the proactive use of early anomaly detection systems. Beyond monitoring, resilience depends on the availability of robust spare-part inventories, adaptive maintenance teams and design provisions that enable rapid recovery after disruptions (IEA, 2022). Adaptation must also be context-specific. In hot and arid regions, failures are commonly caused by high temperatures, strong irradiation and dry conditions; preventive actions include shielding cables from direct exposure, replacing seals regularly and using metal rather than plastic ties. In humid and desert climates, operators face challenges such as potential-induced degradation and accelerated wear due to rapid temperature fluctuations; recommended practices include adjusting inverter settings to local conditions, improving ventilation and frequent filter cleaning (IEA, 2022). In flood-prone areas, elevation of inverters and combiner boxes, IP67-rated materials, reinforced foundations and drainage provisions are key to minimising water ingress and hotspot formation. In cyclone- and storm-prone regions, survival depends on dynamic wind load design, reinforced mounting structures and strict quality control during construction.

Across these contexts, a consistent lesson emerges: resilient PV operation is no longer optional. Extreme weather increasingly shapes the operational reality of European PV plants, requiring O&M strategies to evolve from routine maintenance to climate-adaptive asset management. The challenge is not only to minimise downtime or repair costs, but to ensure that PV generation remains a reliable pillar of Europe's decarbonisation goals under worsening climate stress.

The aim of this paper is to quantify the impact of heatwaves on the operational performance of PV plants in Southern Europe, focusing on Portugal and Spain. The analysis compares measured performance ratios (PR) before, during and after heatwave events with PVsyst simulations based on two meteorological inputs: the TMY and the ERA5-Land reanalysis data set. The study quantifies heatwave impacts on PV performance in Portugal and Spain by comparing observed PR to PVsyst simulations driven by TMY and ERA5-Land, highlighting event-driven losses, limitations of TMY for design under climate change and the added value of reanalysis. By bridging real-world evidence with simulation outputs, the study contributes to the ongoing discussion on how to integrate climate resilience into PV planning and operation in Europe.

2. Methodology

2.1 Sites and data sets

Hourly production data from small/medium-scale PV plants in Southern Europe are used: one in Portugal and two in Spain as shown in Table 1. GHI and air temperature at 2 m time series were extracted from the ERA5-Land (C3S, 2019) reanalysis with hourly resolution and for the grid point closest to the power plant sites. GHI and air temperature for the Amibil site were also available, from a meteorological station of the Agroclimatic Information System for Irrigated Agriculture (SIAR, n.d.). All series are time-zone harmonised (DST-aware). GHI and production data with ERA5-Land GHI < 100W/m^2 are excluded. The data

Table 1. Characteristics of the PV power plants

ID	Name/location	Installed capacity (kWp)	PV modules	Inverters	Mounting	Tilt (º)	Azimuth (º)
1	Zebro/Portugal (37.944; −8.322)	37.06	JAM72S30 545/MR *(545 Wp)*	SUN2000 40KTL M3 *(x1)*	Ground-mounted elevated structure	18º	−30º
2	Ariza/Spain (41.310; −2.060)	15	JAM66S30/MR *(500 Wp)*	SUN2000 6KTL L1 *(x2)*	Ground-mounted	20	10º
3	Amibil/Spain (41.348; −1.645)	64.5	TRINA SOLAR Vertex S+ (R) *(430 Wp)*	SUN2000 KTL M3 36 kW *(x1)* SUN2000 KTL M5 17 kW *(x1)*	Rooftop-mounted	20	−13º

Source(s): Authors' own work

from 28 July 2024, and 29 July 2024, were excluded in Ariza due to failures of the PV plant, with several periods throughout the day when energy production was 0 kWh.

2.2 Event definition and meteorological representativeness

Heatwave windows were obtained from the official bulletins issued by the Spanish State Meteorological Agency (AEMET) for Spain and the Portuguese Institute for Sea and Atmosphere (IPMA) for Portugal, and two were selected per country for analysis which are shown in Table 2.

In all analyses, we define a pre period as the five days immediately preceding each agency-reported heatwave, and a post-period as the five days immediately following it. For each plant and event, we also compute two within-window descriptors to summarise thermal severity: the maximum hourly 2-m air temperature (T_{max}) and cumulative degree-hours above 35°C (*DH35*) as shown in Table 3.

Table 2. Studied heatwaves

Heatwave ID	Country	Start	End	Source
1S	Spain	23 July 2024	1 August 2024	AEMET (2024)
2S	Spain	28 June 2025	30 June 2025	AEMET (2025)
1P	Portugal	15 August 2024	21 August 2024	IPMA (2024)
2P	Portugal	24 May 2025	1 June 2025	IPMA (2025)

Source(s): As shown in the table

Table 3. Heatwave characteristics

Power plant and heatwave ID	T_{max} (ºC)	*DH35* (h)
Amibil_1S	38.9	39
Ariza_1S	37.5	33
Amibil_2S	36.2	13
Ariza_2S	35.9	11
Zebro_1P	39.4	26
Zebro_2P	37.4	16

Source(s): Authors' own work

For both Portugal and Spain, the first episode was harsher at every plant, combining higher peaks (T_{max} up to 38.9°C in Spain, 39.4°C in Portugal) with longer thermal exposure (DH35 up to 39 h in Spain, 26 h in Portugal). Cross-country patterns hint at different stress modes: Spanish events show greater persistence (mean *DH35* of 24 h), while Portuguese plants reach higher temperatures (mean T_{max} of 38.4°C), which may translate into endurance-driven efficiency losses versus peak-temperature risks.

ERA5-Land hourly air temperature and GHI are benchmarked against SIAR for the Amibil location for different regimes (pre-, during and post-heatwave) and for the two Spanish heatwaves, reporting *r*, mean absolute error (MAE), normalised mean bias error (NMBE) and normalised root mean squared error (NRMSE). Normalised metrics use the station mean as divisor. The goal is to quantify representativeness to support ERA5-Land use.

2.3 PVSyst simulations and resilience metrics

Each plant is simulated in PVsyst (8.0.14) under two meteorological drivers: a TMY design case using Meteonorm 8.2 (2000–2019), with site-specific horizon (Meteonorm web service) and a 3D scene for shading, and an actual-meteorology case, driven by ERA5-Land GHI and air temperature. Geometry, loss assumptions, shading and the AC boundary are identical across runs. Outputs are hourly simulated energies using the ERA5-Land and TMY data. As defined in IEC 61724-1, the hourly PR is the observed AC energy divided by the simulated AC energy for the same hour (unitless). We also report a daylight-weighted daily PR aggregated from those hours (IEC, 2021).

To characterise typical performance, a diurnal baseline from the five-day pre-heatwave period was computed as the median PR by hour-of-day and a daily baseline as the mean and standard deviation of the daily values for the same period (analogously for TMY). The mean relative difference between TMY and ERA5-Land daily baselines is also computed (Mean ΔPR_{rel}). During each event, *W*, hourly anomalies relative to the ERA5-Land diurnal baseline for each site are computed as the difference between the hourly PR during the event and the corresponding baseline value at the same hour and three event metrics are derived: drop magnitude (absolute and relative), which is the most negative PR anomaly during the event; time-to-trough (hours from heatwave start to that minimum); and recovery-to-90% (the first hour after the trough when the observed PR returns to at least 90% of its pre-event baseline at the same hour). These metrics use ERA5-Land in the denominator to keep meteorology explicit and isolate asset behaviour. The same metrics are computed for daily PR values.

The cumulative design-expectation gap is quantified with TMY as energy not served (ENS), which is the positive difference between TMY-simulated energy and observed energy, summed over the event window reported in MWh, MWh/MWp and as a percentage of the TMY-simulated energy over the event.

3. Results and discussion

3.1 Site-level validation: ERA5-Land vs in situ

ERA5-Land hourly air temperature and GHI were benchmarked against a co-located station at the Amibil site, restricting validation to daylight hours (ERA5-Land GHI > 100W/m^2, Table 3), showing strong agreement. For air temperature, correlations are high in all regimes, bias is essentially neutral throughout (NMBE between −0.16% and 0.39%), and MAE and NRMSE are small with the only notable exceptions being during and post-2S. In practice, a 2–3°C error translates to only around 1% instantaneous efficiency uncertainty for crystalline-Si (using typical 0.4%/°C–0.5%/°C), so temperature representation is adequate for PV performance modelling. For GHI, skill is very high (up to 0.984) and biases are small, but it is event and regime-dependent, with post-2S showing the weakest agreement.

Figure 1 also summarises the point-by-point agreement between ERA5-Land and the co-located station at Amibil across regimes. Air temperature clusters tightly around the 1:1 line, with most points inside the ±10% corridor consistent with the low MAE and NRMSE. GHI shows larger spread matching the larger NRMSE values and the degradation seen post-2S. These results show a minimal temperature bias and small-to-moderate GHI bias, which indicate that ERA5-Land is representative and appropriate as the meteorological driver for the PVsyst runs and as the reference in the PR-based event metrics.

3.2 Baseline performance

The baseline is the typical diurnal PR for each PV plant, computed from the pre-heatwave window (ERA5-Land driven denominator). A baseline using a TMY-driven denominator is also computed. Figure 2 shows the ERA5-Land baselines by hour of day, while Figure 3 shows the hourly difference between baselines (TMY-ERA5-Land, in PR percentage points). The ERA5-Land diurnal baselines reveal distinct operating signatures. Amibil maintains a high, flat plateau around 95%–98% across the solar peak, Ariza reaches an early maximum and then drifts towards 90%–95% and Zebro operates systematically lower (80%–90%) with a gradual afternoon decline. These shapes frame the later event analysis by fixing the typical hourly performance against which heat-stress anomalies are measured. This is pertinent as Iberian hot extremes are increasing under anthropogenic warming (Vautard *et al.*, 2023; EEA, 2025).

Figure 3 indicates that ERA5-Land and TMY baselines are broadly aligned at mid-day, with the highest differences concentrated near sunrise and sunset. Because these hours yield less energy, hourly differences translate only weakly to the daily-energy weighted PR.

Table 4 reports daily, energy-weighted PR (mean ± standard deviation, SD) for ERA5-Land and TMY together with the relative mean difference. The ERA5-Land daily baselines are internally consistent and narrow. Amibil centres near 95% with small

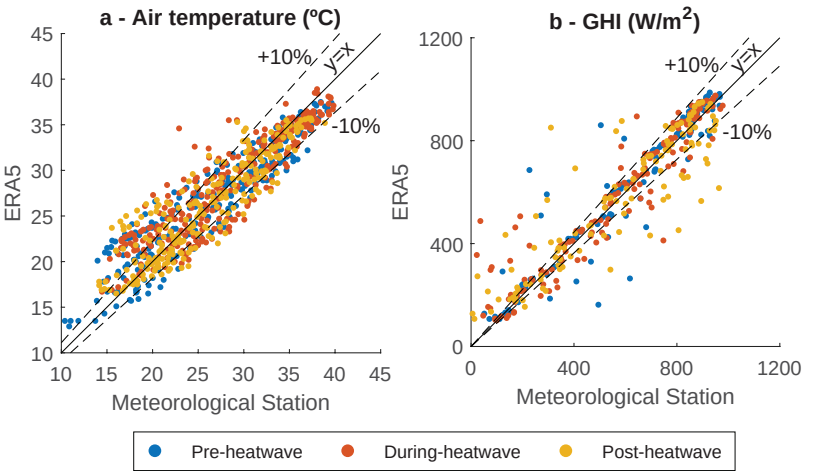

Figure 1. Direct comparison between measured and ERA5-Land air temperature (a) and global horizontal irradiance (b) for both heatwaves and for each regime

Source: Authors' own work

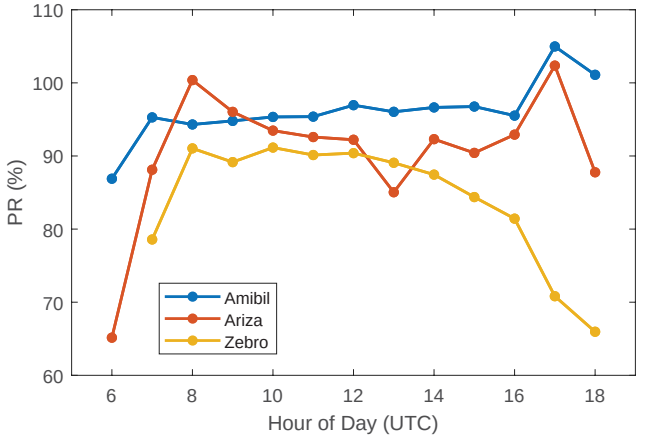

Figure 2. ERA5-Land performance ratio baseline for each photovoltaic plant
Source: Authors' own work

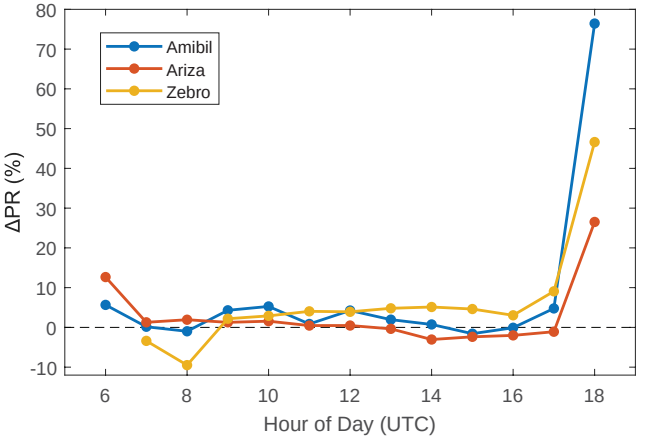

Figure 3. Differences between typical meteorological year and ERA5-Land baselines for each photovoltaic plant
Source: Authors' own work

dispersion, Ariza is slightly lower but also has small dispersion and Zebro operates at lower levels (83%–86%) with broader dispersion reflecting its lower, more sloped diurnal shape. The hourly profile of the baselines (Figure 2) suggests that offsets arise mainly at hours closer to sunrise and sunset, hence their impact on daily, energy-weighted PR is limited but not negligible when deviations are large (2S at Amibil and Zebro). Values above 100% arise because this index is defined as observed energy divided by the TMY simulation for the same period. They simply indicate that the TMY driver underestimates energy in the pre-window (mainly at low sun angles) and do not imply physical PR above 100%.

Table 4. Validation of ERA5-Land air temperature and global horizontal irradiance against station measurements

Variable	Regime	Heatwave	r	NMBE (%)	NRMSE (%)	MAE (ºC)
Air temperature	Pre-heatwave	1S	0.938	0.10	10.65	2.26
		2S	0.935	0.12	10.75	2.32
	Heatwave	1S	0.912	0.02	9.29	2.01
		2S	0.949	0.39	12.52	3.07
	Post-heatwave	1S	0.945	−0.16	8.36	1.72
		2S	0.837	0.29	12.68	2.46
GHI	Pre-heatwave	1S	0.974	8.58	21.68	48.32
		2S	0.920	0.30	33.37	59.90
	Heatwave	1S	0.948	10.42	31.63	57.18
		2S	0.964	−1.21	23.08	58.48
	Post-heatwave	1S	0.984	5.55	16.13	38.77
		2S	0.840	−1.86	59.64	126.83

Source(s): Authors' own work

3.3 Performance under heatwaves

Performance during the events is assessed by hourly and daily PR anomalies relative to the ERA5-Land based diurnal baseline from the pre-event window. Figures 4 through 6 show these anomalies as well as the trough (largest negative anomaly) and the recovery-to-90%. In Table 5, resilience metrics are condensed for hourly and daily data. Large positive spikes at sunrise/sunset reflect the relative anomaly definition at low-sun hours (small hourly baseline/simulated energy), not physical PR > 100%. These points have negligible energy weight and do not affect daily metrics.

Analysing Figure 4 and Table 3 for Amibil, both events exhibit a classic heat-stress signature: troughs occur in the afternoon when module/inverter temperatures peak, followed by rapid recovery as thermal load eases. The deeper but shorter-lived shock in 1S is consistent with its higher thermal severity (Table 6), likely reflecting brief protective derating

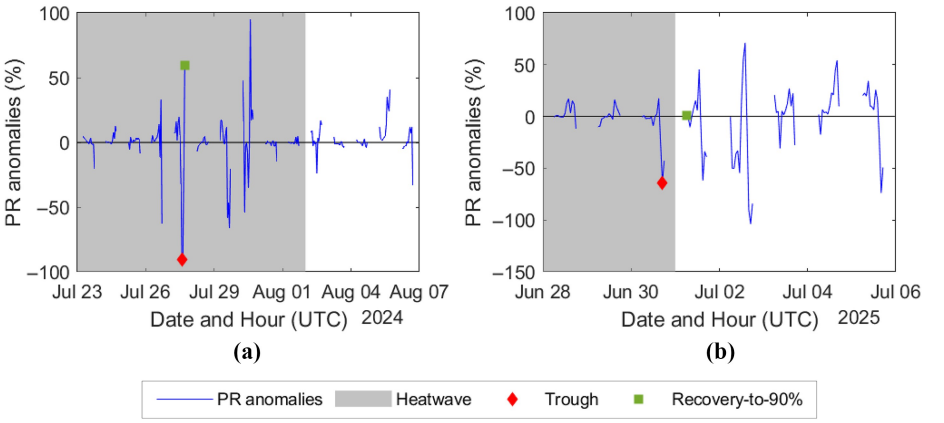

Figure 4. Performance ratio anomalies during and post 1S for Amibil. (a) 1S; (b) 2S
Source: Authors' own work

Table 5. ERA5-Land and typical meteorological year performance ratio baselines (pre-heatwave)

Power plant	Heatwave	ERA5-Land mean ± SD (%)	TMY mean ± SD (%)	Mean ΔPR_{rel} (%)
Amibil	1S	95.38 ± 6.41	93.15 ± 3.27	−2.34
	2S	94.64 ± 2.12	122.03 ± 40.96	28.94
Ariza	1S	94.07 ± 6.35	97.31 ± 12.61	3.44
	2S	88.55 ± 3.84	82.84 ± 5.19	−6.44
Zebro	1P	86.34 ± 14.72	89.41 ± 13.59	3.56
	2P	82.60 ± 9.51	97.67 ± 30.47	18.24

Source(s): Authors' own work

Table 6. Resilience metrics by plant and heatwave (ERA5-Land baseline)

	Power plant	Amibil		Ariza		Zebro	
Timestep	Heatwave	1S	2S	1S	2S	1P	2P
Hourly	$Drop_{max}$ (%)	90.44	63.83	49.52	70.86	20.85	80.31
	$Drop_{max,rel}$ (%)	93.58	60.8	53.29	78.37	31.61	88.85
	Hour of trough (UTC)	14:00	17:00	16:00	15:00	18:00	12:00
	Time-to-trough (h)	110	65	88	63	90	12
	Recovery-to-90% (h)	3	13	1	3	15	2
Daily	$Drop_{max}$ (%)	7.55	3.81	6.5	9.99	1.21†	17.59
	$Drop_{max,rel}$ (%)	7.95	3.96	6.99	10.72	1.29†	21.72
	Time-to-trough (d)	4	2	9	2	7†	0
	Recovery-to-90% (d)	0	0	0	1	0†	1

Note(s): †No negative daily anomaly detected witdin the heatwave window, trough occurs only in the post-event period
Source(s): Authors' own work

near the peak and quick restoration as temperatures fall. In 2S, the trough occurs at 17:00 UTC with 1 h of daylight remaining; because our evaluation uses daylight-only hours, the reported recovery-to-90% includes the overnight gap and should not be interpreted as a slower physical response. This pattern is consistent with temperature-driven efficiency loss and inverter thermal derating near peak component temperatures (Ebhota and Tabakov, 2022; De Lima *et al.*, 2023). Amibil's flat, high midday baseline means sunrise/sunset anomalies carry reduced energy weight, so large hourly excursions compress into small daily deficits. At the daily scale, both events show single-digit drops that peak on Day 4 (1S) and Day 2 (2S) and recover within the same day, indicating that heat-related risk is concentrated in a handful of hot afternoon hours rather than sustained multi-day degradation.

Ariza's response mirrors its baseline signature as shown in Figure 5 (early peak followed by an afternoon drift), with PR anomalies clustering near zero for much of the window but having extreme values in mid-afternoon, when thermal load and inverter temperatures are highest. In 1S, the drop is moderate and short-lived, with an almost immediate rebound once the peak passes, which is consistent with brief protective derating rather than sustained loss. By contrast, 2S shows a deeper trough and a slower intra-day recovery, even though its thermal severity is lower (Table 6). This inversion suggests that factors such as inverter derating thresholds, transient curtailment or weaker convective cooling, dominated over meteorology in determining the depth and duration of the dip. Such plant-specific sensitivity

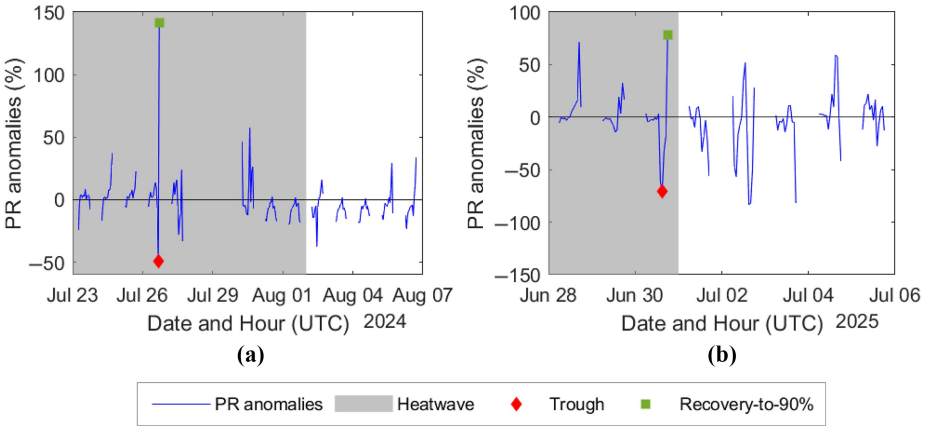

Figure 5. Performance ratio anomalies during and post-heatwave for Ariza. (a) 1S; (b) 2S
Source: Authors' own work

accords with PV vulnerability literature and O&M guidance (Patt *et al.*, 2013; IEA, 2022). At the daily scale, losses remain single-digit and short-lived (Table 5), reinforcing that risk at Ariza is hour-centric, concentrated in hot afternoon hours rather than a multi-day decline.

Zebro behaves in line with its sloping afternoon baseline, as seen in Figure 6. In 1P, Zebro's hourly anomaly has a convex diurnal shape, slightly positive at midday and negative towards sunrise/sunset, while the hourly trough occurs late afternoon and resolves the next day. Because the negative hours coincide with low irradiance, the daily aggregate does not turn negative during the heatwave period (†in Table 5 marks the daily minimum just after the heatwave). In 2P, however, the trough occurs near solar noon, carries high energy weight and translates into a daily drop on Day 1 with recovery within that day. Thus, at Zebro the deficit is not systematically midday centred.

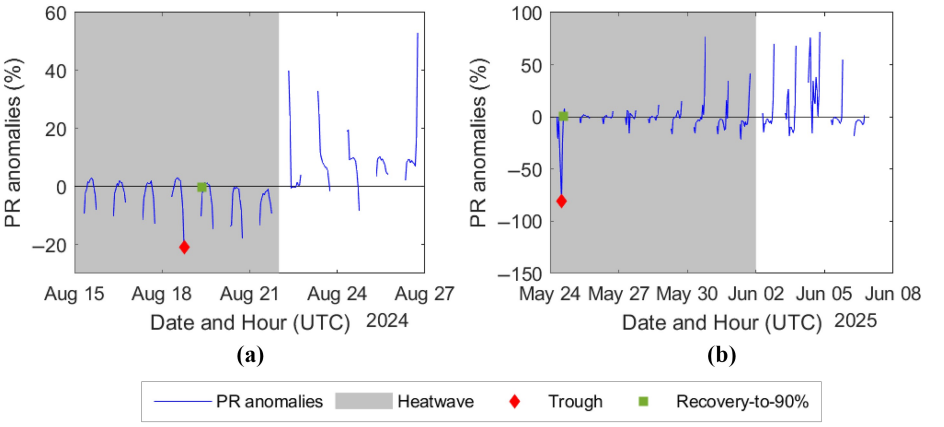

Figure 6. Performance ratio anomalies during and post-heatwave for Zebro. (a) 1P; (b) 2P
Source: Authors' own work

Across the three plants the response is hour-centric (sharp troughs with intra-day recovery), but the magnitude and day-level impact depend on each site's baseline and on when within the diurnal cycle the minimum occurs. The intra-day drops and recoveries observed even in the post-heatwave regimes indicate that the proximate driver of hourly PR deficits is not the label "heatwave" *per se*, but short-lived exceedance of thermal thresholds (high air temperature with limited wind cooling) that triggers protective derating and then normalisation once thermal load eases. As Western European heat extremes intensify, such hot-hour risks will occur more often in Iberia (Vautard *et al.*, 2023; Dong and Sutton, 2025; EEA, 2025). This is consistent with PV temperature physics, where module temperature responds to irradiance, ambient temperature and wind speed, and with evidence that inverters thermally derate under high component/ambient temperatures; hence, acute afternoon spikes can produce the same signature inside or outside officially declared heatwaves.

3.4 Typical meteorological year design gap

Table 7 quantifies the ENS when TMY is used as the driver, i.e. the energy that TMY-based design would expect but was not delivered in operation. In all cases these values are non-zero, but their magnitude and timing vary widely across plants. In absolute terms and per-kWp, the largest gaps occur at Zebro-2P, Amibil-1S and Amibil-2S. As a share of simulated energy, the largest relative shortfall is Ariza-2S, followed by Zebro-2P and Amibil-2S. The regime split is also site and heatwave dependent. During-event losses dominate at Amibil-1S, Zebro-1P and Zebro-2P, while post-event losses are the largest component for Amibil-2S and Ariza-2S. This indicates that TMY-only simulations can overestimate both during and, in some cases, after the event. This aligns with evidence that TMY under-represents extremes and so event-centred stress tests are warranted (Loon *et al.*, 2020; Perera *et al.*, 2020). Within this limited sample (three plants, four events), the data show that the size and timing of the TMY gap are plant-specific and event-specific, reinforcing the need to complement TMY with event-centred analyses when assessing operational risk. Future hot-hour frequencies can be quantified using high-resolution climate projections (Gutowski *et al.*, 2020).

4. Conclusions

Heatwaves, projected to intensify across Iberia, pose operational risks for PV plants. We assessed three Iberian plants across four agency-declared events by pairing observed energy with ERA5-Land-driven and TMY PVsyst simulations in an event-centred framework. ERA5-Land reproduced site meteorology well at the validated site (air temperature r = 0.91–0.95; GHI up to 0.98), supporting its use as the denominator for PR metrics. Pre-event PR baselines revealed distinct operating signatures, which shaped event responses by fixing

Table 7. Energy not served with typical meteorological year

Power plant	Heatwave	During heatwave			Post-heatwave			Total		
		kWh	kWh/kWp	% of E_{sim}	kWh	kWh/kWp	% of E_{sim}	kWh	kWh/kWp	% of E_{sim}
Amibil	1S	414.54	27.64	11.29	83.23	5.55	4.21	497.77	33.18	8.81
	2S	68.02	4.53	5.24	399.57	26.64	18.29	467.58	31.17	13.43
Ariza	1S	59.02	3.93	8.51	59.09	3.94	12.94	118.11	7.87	10.27
	2S	65.91	4.39	21.4	108.18	7.21	22.96	174.09	11.6	22.34
Zebro	1P	206.19	13.74	13.42	56.52	3.77	5.21	262.70	17.51	10.02
	2P	342.99	22.87	15.94	210.26	14.02	20.07	553.25	36.88	17.30

Source(s): Authors' own work

the typical hourly performance against which heat-stress anomalies were measured. Across events, impacts were hour-centric: sharp afternoon PR troughs with intra-day recovery. The deepest hourly loss reached 90.44% (Amibil-1S), and the largest daily loss was 17.59% (Zebro-2P) with recovery within 0–1 days. TMY expectations overestimated energy in all cases, with the largest absolute gap at Zebro-2P and the highest relative gap at Ariza-2S. In planning and contracting terms, this means design-year expectations systematically understate heat-related operational risk. Intra-day drops and recoveries also occurred outside official heatwave windows, indicating that brief exceedances of thermal thresholds, not the label "heatwave" *per se*, drive loss concentration in hot hours. These findings are bounded by scope (three plants, four events, *in situ* validation at one site) and by comparing a stationary TMY (2000–2019) with 2024–2025 conditions. Even so, the message for European deployment is practical and climate-relevant. Complement TMY with event-centred stress tests using reanalysis or site-calibrated data, specify and operate for hot-hour resilience (thermal headroom, ventilation, derating management, rapid post-event inspection) and recognise in adequacy and contracts that short, frequent hot-hour losses will occur more often as the climate warms.

The metrics developed here provide actionable triggers for today's decisions. Developers can use ENS and trough timing to set minimum thermal headroom and ventilation/layout requirements in procurement. Operators can codify hot-hour protocols (derating thresholds, rapid post-event inspection) and report ENS alongside PR during extreme heat to make losses visible in dashboards. Planners and regulators can account for more frequent hot-hour deficits in adequacy and reserve margins, recognising that typical-year expectations systematically understate risk as the climate warms. These actions are implementable with existing SCADA data and reanalysis forcing. Scaling the framework across plant typologies and regions and coupling it with high-resolution climate projections will quantify how often high-risk hot hours are likely to occur, enabling measurable resilience gains in procurement, design reviews and operational dashboards.

References

Abdelmalak, M., Cox, J., Ericson, S., Hotchkiss, E. and Benidris, M. (2023), "Quantitative Resilience-Based assessment framework using EAGLE-I power outage data", *IEEE Access*, Vol. 11, pp. 7682-7697, doi: 10.1109/ACCESS.2023.3235615.

AEMET (2024), "Julio de 2024, un mes muy cálido y muy seco [July 2024, a very warm and very dry month]", available at: www.aemet.es/es/noticias/2024/08/informe-julio-2024.pdf (accessed 18 August 2025).

AEMET (2025), "Resumen mensual climatológico junio 2025 [Climatological monthly summary June 2025]", available at: www.aemet.es/documentos/es/serviciosclimaticos/vigilancia_clima/resumenes_climat/mensuales/2025/res_mens_clim_2025_06.pdf (accessed 18 August 2025).

Añel, J., Pérez-Souto, C., Bayo-Besteiro, S., Prieto-Godino, L., Bloomfield, H., Troccoli, A. and Torre, L. (2024), "Extreme weather events and the energy sector in 2021", *Weather, Climate, and Society*, Vol. 16 No. 3, pp. 353-368, doi: 10.1175/wcas-d-23-0115.1.

Ascencio-Vásquez, J., Kaaya, I., Brecl, K., Weiss, K. and Topic, M. (2019), "Global climate data processing and mapping of degradation mechanisms and degradation rates of PV modules", *Energies*, Vol. 12 No. 24, p. 4749, doi: 10.3390/en12244749.

Ataman, A. and Arslanoğlu, N. (2024), "Investigation of the cooling effect of wind on rooftop PV power plants", *Case Studies in Thermal Engineering*, Vol. 63, p. 105295, doi: 10.1016/j.csite.2024.105295.

Bamisile, O., Acen, C., Cai, D., Huang, Q. and Staffell, I. (2025), "The environmental factors affecting solar photovoltaic output", *Renewable and Sustainable Energy Reviews*, Vol. 208, p. 115073, doi: 10.1016/j.rser.2024.115073.

Bošnjaković, M., Stojkov, M., Katinić, M. and Lacković, I. (2023), "Effects of extreme weather conditions on PV systems", *Sustainability*, Vol. 15 No. 22, doi: 10.3390/su152216044.

Brennan, K., Thurnnerr, I., Sprenger, M. and Wernli, H. (2025), "Insights from hailstorm track analysis in European climate change simulations", *EGUsphere*, doi: 10.5194/egusphere-2025-918.

Chakraborty, S., Haldkar, A. and Kumar, N. (2023), "Analysis of hail impact on the performance of commercially available photovoltaic modules with different front glass thickness", *Renewable Energy*, Vol. 203, pp. 345-356, doi: 10.1016/j.renene.2022.12.061.

Chen, Y., Liu, Y., Tian, Z., Dong, Y., Zhou, Y., Wang, X. and Wang, D. (2019), "Experimental study on the effect of dust deposition on photovoltaic panels", *Energy Procedia*, Vol. 158, pp. 483-489, doi: 10.1016/j.egypro.2019.01.139.

Copernicus Climate Change Service (C3S) (2019), *ERA5-Land Hourly Data from 1950 to Present, Climate Data Store (CDS)*, C3S, doi: 10.24381/cds.e2161bac.

Corwin, K., Burkhardt, J., Corr, C., Stackhouse, P., Munshi, A. and Fischer, E. (2025), "Solar energy resource availability under extreme and historical wildfire smoke conditions", *Nature Communications*, Vol. 16 No. 1, doi: 10.1038/s41467-024-54163-8.

De Lima, G., Ribeiro, A., Lemos, F., Silveira, J., Barros, T. and Villalva, M. (2023), "Comparing temperature derating test in the laboratory with commercial photovoltaic inverter datasheet", 2023 IEEE 8th Southern Power Electronics Conference and 17th Brazilian Power Electronics Conference (SPEC/COBEP), *Florianopolis, Brazil*, pp.1-7, doi: 10.1109/SPEC56436.2023.10407835.

Dehghani, F., Mohammadi, M. and Karimi, M. (2023), "Age-dependent resilience assessment and quantification of distribution systems under extreme weather events", *International Journal of Electrical Power and Energy Systems*, Vol. 150, p. 109089, doi: 10.1016/j.ijepes.2023.109089.

Dong, B. and Sutton, R. (2025), "Drivers and mechanisms contributing to excess warming in Europe during recent decades", *Npj Climate and Atmospheric Science*, Vol. 8 No. 1, doi: 10.1038/s41612-025-00930-3.

Dwivedi, D., Babu, K., Yemula, P., Chakraborty, P. and Pal, M. (2025), "A comprehensive metric for resilience evaluation in electrical distribution systems under extreme conditions", *Applied Energy*, Vol. 380no, p. 125001, doi: 10.1016/j.apenergy.2024.125001.

Ebhota, W. and Tabakov, P. (2022), "Influence of photovoltaic cell technologies and elevated temperature on photovoltaic system performance", *Ain Shams Engineering Journal*, Vol. 14 No. 7, p. 101984, doi: 10.1016/j.asej.2022.101984.

EEA (2021), "Hail", available at: www.eea.europa.eu/data-and-maps/indicators/hail/assessment (accessed 18 August 2025).

EEA (2025), "Global and European temperatures", available at: www.eea.europa.eu/en/analysis/indicators/global-and-european-temperatures (accessed 18 August 2025).

Ekisheva, S., Dobson, I., Rieder, R. and Norris, J. (2022), "Assessing transmission resilience during extreme weather with outage and restore processes", 2022 17th International Conference on Probabilistic Methods Applied to Power Systems (PMAPS), *Manchester, United Kingdom*, pp.1-6, doi: 10.1109/PMAPS53380.2022.9810645.

Ford, E., Peters, I.M. and Hoex, B. (2024), "Quantifying the impact of wildfire smoke on solar photovoltaic generation in Australia", *iScience*, Vol. 27 No. 2, doi: 10.1016/j.isci.2023.108611.

Fregosi, D. and Bolen, M. (2022), "An evaluation of empirical models for use in normalizing PV plant performance data", 2022 IEEE 49th Photovoltaics Specialists Conference (PVSC), *Philadelphia, PA, USA*, pp. 116-120, doi: 10.1109/PVSC48317.2022.9938822.

Gahlot, S. (2024), "Catching the sun: adapting solar power to the challenges of climate change", available at: www.swissre.com/institute/research/topics-and-risk-dialogues/climate-and-natural-catastrophe-risk/climate-change-solar-power.html (accessed 18 August 2025).

Ghosh, P. and De, M. (2022), "Probabilistic quantification of distribution system resilience for an extreme event", *International Transactions on Electrical Energy Systems*, Vol. 2022, doi: 10.1155/2022/3838695.

Gilletly, S., Jackson, N. and Staid, A. (2023), "Evaluating the impact of wildfire smoke on solar photovoltaic production", *Applied Energy*, Vol. 348, p. 121303, doi: 10.1016/j.apenergy.2023.121303.

Gutowski, W., Ullrich, P., Hall, A., Leung, L., O'Brien, T., Patricola, C., Arritt, R., Bukovsky, M., Calvin, K., Feng, Z., Jones, A., Kooperman, G., Monier, E., Pritchard, M., Pryor, S., Qian, Y., Rhoades, A., Roberts, A., Sakaguchi, K., Urban, N. and Zarzycki, C. (2020), "The ongoing need for High-Resolution regional climate models: process understanding and stakeholder information", *Bulletin of the American Meteorological Society*, Vol. 101 No. 5, pp. E664-E683, doi: 10.1175/bams-d-19-0113.1.

Hameed, M., Daßler, D., Alias, Q., Scheer, R. and Gottschalg, R. (2024), "Economic consequences based on reversible and irreversible degradation of PV park in the harsh climate conditions of Iraq", *Energies*, Vol. 17 No. 11, p. 2652, doi: 10.3390/en17112652.

Han, H., Ge, Y., Wang, Q., Chen, X., Yang, Q., Tian, L. and Xen, X. (2025), "Impact of extreme weather on the reliability of building distributed energy systems – A case study in three cities in China", *Renewable and Sustainable Energy Reviews*, Vol. 212, p. 115374, doi: 10.1016/j.rser.2025.115374.

Hudișteanu, V.-S., Cherecheș, N.-C., Turcanu, F.-E., Hudișteanu, I. and Romila, C. (2024), "Impact of temperature on the efficiency of monocrystalline and polycrystalline photovoltaic panels: a comprehensive experimental analysis for sustainable energy solutions", *Sustainability*, Vol. 16 No. 23, p. 10566, doi: 10.3390/su162310566.

Husain, S., Shukla, A., Bharsakade, R., Prabhakar, P., Vijayaraghavan, P., Sherje, N. and Tarigonda, H. (2024), "Thermal management strategies in High-Power energy storage device", *E3S Web of Conferences*, Vol. 591, doi: 10.1051/e3sconf/202459105012.

IEA (2022), "Guidelines for operation and maintenance of photovoltaic power plants in different climates", available at: https://iea-pvps.org/wp-content/uploads/2022/11/IEA-PVPS-Report-T13-25-2022-OandM-Guidelines.pdf (accessed 18 August 2025).

IEA (2025), "Snapshot of global PV markets 2025", available at: https://iea-pvps.org/snapshot-reports/snapshot-2025/ (accessed 18 August 2025).

IEC (2021), *IEC 61724-1:2021 Photovoltaic System Performance — Part 1: Monitoring*, International Electrotechnical Commission, Geneva.

IPCC (2022), "Climate change 2022: impacts, adaptation and vulnerability", available at: www.ipcc.ch/report/ar6/wg2/ (accessed 18 August 2025).

IPMA (2024), "Boletim climático Portugal continental agosto 2024 [mainland Portugal climate bulletin august 2024]", available at: www.ipma.pt/resources.www/docs/im.publicacoes/edicoes.online/20240920/mOsOBinMxFgmijKMgynf/cli_20240801_20240831_pcl_mm_co_pt.pdf (accessed 18 August 2025).

IPMA (2025), "Boletim climático Portugal continental Maio 2025 [mainland Portugal climate bulletin may 2025]", available at: www.ipma.pt/resources.www/docs/im.publicacoes/edicoes.online/20250616/IvWmkgTamdGgZQUYxJoU/cli_20250501_20250531_pcl_mm_co_pt.pdf (accessed 18 August 2025).

Islam, M., Jadin, M., Mansur, A. and Alharbi, T. (2024), "Electrical performance and degradation analysis of Field-Aged PV modules in tropical climates: a comparative study", *Energy Conversion and Management: X*, Vol. 24, p. 100719, doi: 10.1016/j.ecmx.2024.100719.

Jimba, C., Akimoto, Y. and Okajima, K. (2025), "Assessment methodology for the resilience of energy systems in positive energy buildings", *E-Prime - Advances in Electrical Engineering, Electronics and Energy*, Vol. 11, p. 100908, doi: 10.1016/j.prime.2025.100908.

Kahraman, A., Kendon, E. and Fowler, H. (2024), "Climatology of severe hail potential in Europe based on a convection permitting simulation", *Climate Dynamics*, Vol. 62, p. 6625-6642, doi: 10.1007/s00382-024-07227-w.

Kim, G., Choi, J., Park, S., Bhang, B., Nam, W., Cha, H., Park, N. and Ahn, H. (2019), "Prediction model for PV performance with correlation analysis of environmental variables", *IEEE Journal of Photovoltaics*, Vol. 9 No. 3, pp. 832-841, doi: 10.1109/JPHOTOV.2019.2898521.

Lei, X. and Xu, X. (2024), "Climate crisis on energy bills: who bears the greater burden of extreme weather events?", *Economics Letters*, Vol. 247, p. 112103, doi: 10.1016/j.econlet.2024.112103.

Loon, A., Chattopadhyay, D. and Bazilian, M. (2020), "Atypical variability in TMY-based power systems", *Energy for Sustainable Development*, Vol. 54, pp. 139-147, doi: 10.1016/j.esd.2019.09.004.

Meslier, V., Chambion, B., Bouchard, P. and Bouvard, J. (2024), "Thermal expansion behavior of a thermoplastic polyolefin for photovoltaic application over hygrothermal aging", *IEEE Journal of Photovoltaics*, Vol. 14 No. 6, pp. 920-929, doi: 10.1109/JPHOTOV.2024.3463950.

Okonkwo, P., Nwokolo, S., Udo, S., Obiwulu, A., Onnoghen, U., Alarifi, S., Eldosouky, A., Ekwok, S., Andráš, P. and Akpan, A. (2025), "Solar PV systems under weather extremes: case studies, classification, vulnerability assessment, and adaptation pathways", *Energy Reports*, Vol. 13, pp. 929-959, doi: 10.1016/j.egyr.2024.12.067.

Omazic, A., Oreski, G., Halwachs, M., Eder, G., Hirschl, C., Neumaier, L., Pinter, G. and Erceg, M. (2019), "Relation between degradation of polymeric components in crystalline silicon PV module and climatic conditions: a literature review", *Solar Energy Materials and Solar Cells*, Vol. 192, pp. 123-133, doi: 10.1016/J.SOLMAT.2018.12.027.

Panteli, M., Mancarella, P., Trakas, D., Kyriakides, E. and Hatziargyriou, N. (2017), "Metrics and quantification of operational and infrastructure resilience in power systems", *IEEE Transactions on Power Systems*, Vol. 32 No. 6, pp. 4732-4742, doi: 10.1109/TPWRS.2017.2664141.

Patt, A., Pfenninger, S. and Lilliestam, J. (2013), "Vulnerability of solar energy infrastructure and output to climate change", *Climatic Change*, Vol. 121 No. 1, pp. 93-102, doi: 10.1007/s10584-013-0887-0.

Perera, A., Nik, V., Chen, D., Scartezzini, J. and Hon, T. (2020), "Quantifying the impacts of climate change and extreme climate events on energy systems", *Nature Energy*, Vol. 5 No. 2, pp. 150-159, doi: 10.1038/s41560-020-0558-0.

Pierce, B., Wieser, R., Ciardi, T., Yao, A., French, R., Bruckman, L. and Li, M. (2024), "Comparison of empirical and data driven digital twins for a PV+battery fleet", 2024 IEEE 52nd Photovoltaic Specialist Conference (PVSC), Seattle, WA, USA, pp.1391-1397. 10.1109/PVSC57443.2024.10749422.

Pizzimbone, L. and Jrad, F. (2023), "reXplan: a novel tool for the analysis of climate resilience in power systems", 2023 IEEE PES Innovative Smart Grid Technologies Europe (ISGT EUROPE), pp.1-6. 10.1109/ISGTEUROPE56780.2023.10408548.

Poddar, S., Rougieux, F., Evans, J., Kay, M., Prasad, A. and Bremner, S. (2024), "Accelerated degradation of photovoltaic modules under a future warmer climate", *Progress in Photovoltaics: Research and Applications*, Vol. 32 No. 7, pp. 456-467, doi: 10.1002/pip.3788.

Rady, M., Muhammad, M. and Shahid, S. (2025), "Evolving typical meteorological year (TMY) data for building energy simulation: a comprehensive review of methods, challenges, and future directions", *Advances in Building Energy Research*, Vol. 19 No. 3, pp. 269-299, doi: 10.1080/17512549.2025.2457649.

Razak, A., Irwan, Y., Leow, W., Irwanto, M., Safwati, I. and Zhafarina, M. (2016), "Investigation of the effect temperature on photovoltaic (PV) panel output performance", *International Journal on Advanced Science, Engineering and Information Technology*, Vol. 6 No. 5, pp. 682-688, doi: 10.18517/IJASEIT.6.5.938.

Rettie, F., Gayler, S., Weber, T., Tesfaye, K. and Streck, T. (2023), "High-resolution CMIP6 climate projections for Ethiopia using the gridded statistical downscaling method", *Scientific Data*, Vol. 10 No. 1, p. 442, doi: 10.1038/s41597-023-02337-2.

Ruosteenoja, K. and Jylha, K. (2023), "Heatwave projections for Finland at different levels of global warming derived from CMIP6 simulations", *Geophysica*, Vol. 58 No. 1, pp. 47-75.

SiAR (n.d), "Sistema de información agroclimática Para el regadío [agroclimatic information system for irrigated agriculture]", available at: https://servicio.mapa.gob.es/websiar/SeleccionParametrosMap.aspx?dst=1 (accessed 18 August 2025).

Sun, F., Li, L., Bian, D., Ji, H., Li, N. and Wang, S. (2024), "Short-term PV power data prediction based on improved FCM with WTEEMD and adaptive weather weights", *Journal of Building Engineering*, Vol. 90, p. 109408, doi: 10.1016/j.jobe.2024.109408.

Vautard, R., Cattiaux, J., Happé, T., Singh, J., Bonnet, R., Cassou, C., Coumou, D., D'Andrea, F., Faranda, D., Fischer, E., Ribes, A., Sippel, S. and Yiou, P. (2023), "Heat extremes in Western Europe increasing faster than simulated due to atmospheric circulation trends", *Nature Communications*, Vol. 14 No. 1, p. 6803, doi: 10.1038/s41467-023-42143-3.

Zhang, M., Han, Y., Wang, C., Yang, P., Wang, C. and Zalhaf, A. (2024), "Ultra-short-term photovoltaic power prediction based on similar day clustering and temporal convolutional network with bidirectional long short-term memory model: a case study using DKASC data", *Applied Energy*, Vol. 375, p. 124085, doi: 10.1016/j.apenergy.2024.124085.

Corresponding author
Sara Pereira can be contacted at: spereira@uevora.pt